Atmospheric Mesoscale Spectra and Structure Functions of Mean Horizontal Velocity Fluctuations Measured with a Doppler Sodar Network

M. MASMOUDI AND A. WEILL

CNET/CRPE/CNRS, Issy les Moulineaux, France*

(Manuscript received 2 May 1987, in final form 28 December 1987)

ABSTRACT

Analyses of mean horizontal wind speed from four Doppler sodars separated by 15 to 38 km in the Gers region during the Mesogers 84 experiment gave information on the horizontal wind speed spectral behavior of the so-called mesoscale turbulence during 3 days of fair weather situations. The $-5/3$ spectral behavior is obtained. A study of the validity of the Taylor hypothesis at this scale shows that for the scales that are considered, this hypothesis is reasonable, but poses difficult questions about the transport speed, which seems to be close to the mean wind speed spatially averaged over the four sodars.

Vorticity spectra are found to support a vortical mode related to quasi-two-dimensional turbulence rather than due to purely internal inertia-gravity wave interactions.

1. Introduction

Atmospheric spectral behavior of horizontal wind velocity for scales larger than small-scale turbulence are very important for use in diffusion and horizontal transport problems and numerical modeling. However, knowledge in this field is far from being definitive and many theoretical and experimental studies show or suggest different spectral behavior or different theoretical justifications.

Regarding horizontal scales of turbulence, we adopt the usual classification from which the small scale is smaller than a few kilometers, the mesoscale is larger than a few kilometers and smaller than 1000 km, and the large scale is larger than 1000 km.

Several theoretical models show spectral domains in which the spectral energy is varying in $k^{-5/3}$ or k^{-3} where k is the wavenumber (Kraichnan 1967; Lorenz 1969; Leith and Kraichnan 1972). The k^{-3} law is related to the enstrophy (square of the vorticity) inertial range on the macroscale of turbulence.

Some experimental studies (Julian et al. 1970; Desbois 1975) have shown a k^{-3} spectral behavior for large scales: $2\pi/k > 1000$ km. This spectral behavior has been also found and justified by Morel and Larchevèque (1974) for scales smaller than 1000 km. Gage (1979) and Nastrom and Gage (1983, 1984), have shown that the $k^{-5/3}$ behavior was valid for "mesoscales" smaller than 1000 km. For small scale turbulence, the $k^{-5/3}$ behavior predicted by the theory of three-dimensional local random isotropic turbulence of Kolmogorov is found and applied, corresponding to an "inertial subrange" in which energy is transferred toward small scales of motion. For mesoscales, the inverse cascade corresponding to two-dimensional turbulence is often argued to justify mesoscale spectral behavior. Gage and Jasperson (1979), studying the temporal structure function, have also discussed the validity of the space–time equivalence for mesoscale turbulence (Taylor's hypothesis).

The complex terrain Mesogers 1984 experiment took place in southwest France and was devoted to the study of atmospheric boundary layer and flux measurements at different temporal and spatial scales (Weill et al. 1987). Four Doppler sodars were used, from which energy spectra of mean horizontal wind speed and structure functions of mean velocity fluctuations were computed.

After a short development of the theories to be tested and a description of the experiment and dataset, the energy spectral behavior as a function of a frequency and temporal structure functions will be discussed. Then we shall try to compare the spatial and temporal behavior of structure functions. In the Conclusions, we shall demonstrate the difficulty in identifying the contribution of phenomena to spectral behavior.

2. The theories to be tested

Different theories have provided evidence for the existence of a $k^{-5/3}$ law for mesoscales of turbulence

* CNET: Centre National d'Etudes et Télécommunications; CRPE: Centre National de Recherches sur l'Environnement; and CNRS: Centre National de la Recherche Scientifique.

Corresponding author address: Dr. Alain Weill, CNET/CRPE/CNRS, 38–40 Ave. du General Leclerc, 92131, Issy les Moulineaux, France.

and two major theories have been proposed to explain the relevance of this $-5/3$ exponent of the energy spectrum. Gage (1979) proposed a theory which has been experimentally verified in a wind channel by Dickey and Mellor (1980), assuming that in a well-mixed flow, the three-dimensional isotropic turbulence can collapse and be followed by internal gravity waves. In this case, in the absence of kinetic energy dissipation, gravity waves determine vertical velocity fluctuations, though mean flow organization remains unchanged. In these conditions two-dimensional turbulence can appear and interact with gravity waves. This theory of collapse of three-dimensional turbulence has been extended by Lilly (1983) suggesting that such a behavior gives an explanation to the mesoscale turbulence between horizontal scales from a few kilometers up to several hundred of kilometers (Lesieur 1983).

On the contrary, Van Zandt (1982) follows the concepts proposed by Garrett and Munk (1979) to rationalize oceanic energy spectra based on the theoretical dispersion of inertia–gravity waves. However, as suggested by Lilly (1984) it is difficult to verify these hypotheses in the troposphere, and in the comparison of the atmosphere and ocean, it is not relevant to ignore properties such as compressibility and radiative exchange.

It is interesting to note that the difficulty for gravity waves to transport vorticity could justify one theory rather than another.

The first thing to test is, indeed, the validity of the turbulence spectrum behavior as described by the last two theories and also to analyze with sodar data the space–time equivalence suggested by Gage and Jasperon (1979), and Gage (1979). For that purpose two different functions will be computed.

- The energy spectrum: using the Fourier transform of the different types of fluctuations:

$$E(f) = \frac{1}{T}\left|\int_{-\infty}^{\infty} v(t)\exp(-2\pi i f t)dt\right|^2$$

where T is the finite length of the record, f the frequency and v the signal.

- The temporal structure function of velocity fluctuations, which is defined by $D(\tau) = \overline{(v(\tau) - v(t+\tau))^2}$ where τ is the lag time; this has the advantage of being dependent only on the lag time (Tatarski 1961). Notice that if the structure function is in the form $Dv(\tau) = A\tau^a$, it is equivalent to the spectral form $A1\, f^{-a-1}$ for the statistics of turbulence met by the previous authors, where f is a frequency and $A1$ a constant.

The Taylor transformation relating time and space, as discussed for mesoscale turbulence by Gage and Jasperon (1979), poses the question of mesoscale turbulent transport; we shall test the relationships between temporal and spatial structure functions searching for what the transport velicity $\langle V\rangle$ corresponds to in the relationship between temporal and spatial structure function:

$$Dv(\tau) = A\langle V\rangle^{-a}\delta r^a$$

when the temporal and spatial structure functions follow, respectively, a τ^a and a δr^a power law.

3. The dataset

Data analyzed in this paper come from the Mesogers 84 experiment (Weill et al. 1987), which took place from 9 September to 5 October 1984 in the hilly region of Gers, which is in the southwest of France, 150 km from Bordeaux. During this campaign, seven monostatic, three-antennae Doppler sodars were used, four of which were working routinely during the whole experiment. We are concerned here with these four Doppler sodars and mean horizontal wind speed data obtained during September 26–28 corresponding to a fair weather situation without precipitation. Distances between the sodars stations ranged from 15 to 38 km. A map with sodars locations can be found in Fig. 1. The sodars characteristics are as follows.

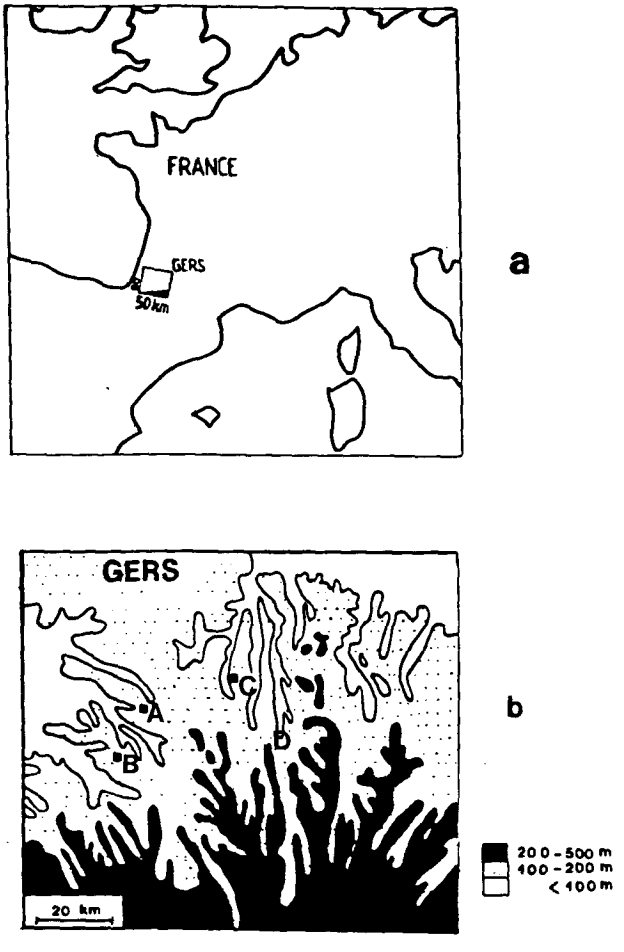

FIG. 1. Gers region and sodar locations.

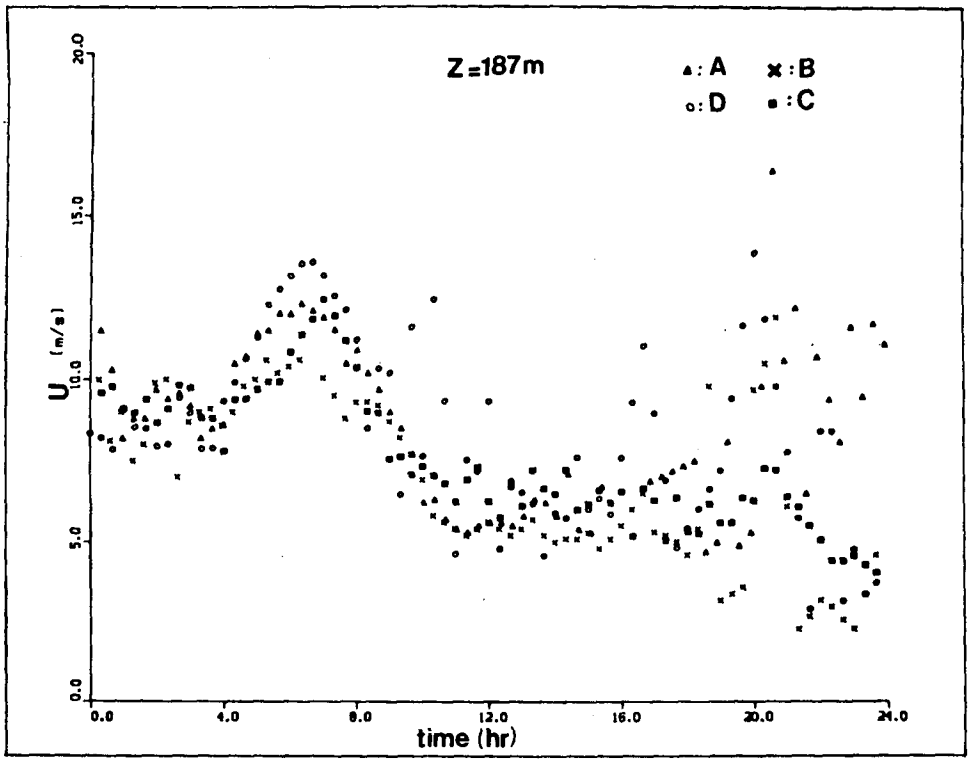

FIG. 2. (a) Wind speed and direction times series for the four Doppler sodars: A, Ayzieu (CRPE); B, Magnan (CRPE); C, Ramouzens (KNMI); D, Lauraèt (EDF); on 26 September, 1984. (b) As in (a) for wind direction.

Sodars A and B (Weill et al. 1978, 1980) use an acoustic frequency of 2000 Hz and give wind information for gates ranging from 22 up to 540 m. These sodars are not commercial systems but have been designed at C.R.P.E. Sodar C from E.D.F.* and sodar D from K.N.M.I.† are commercial systems and use two frequencies (1600 and 2000 Hz). Wind information is generally obtained from 25 to 500 m. In this study we shall analyze spectra of mean horizontal wind speeds averaged over 20 min. To assure better accuracy in the results, only data associated with large signal-to-noise ratio are used, which limits the observation range to a 350-m height. For sodars A and B comparisons with in situ measurements (Chong 1976), and theoretical considerations (Spizzichino 1974) have shown that wind speed uncertainty is close to 0.5 m s^{-1} for winds averaged over 20 min. For the commercial sodars systems C and D, an uncertainty of 1 m s^{-1} can be considered. A comparison between wind speed evolution for the four sodars during the three days of this analysis (Fig. 2) shows that the wind speed patterns for 26 September are very similar. The horizontal wind spectra obtained can, at least, be considered to come from comparable sensors observing simultaneously at several locations. There are, indeed, time periods during which the horizontal wind velocity differences are sufficiently small to be negligible. However, there are several time periods during which the curves of horizontal wind speed evolution are quite different, suggesting that there is not bias but rather significative differences between the various sodars.

4. Spectral density and structure functions

Spectra of horizontal wind speed are obtained from Fourier transform of the horizontal wind speed averaged over 20 minutes. Due to the effect of finite duration of the atmospheric wind signal on the spectrum, a Papoulis (1973) window was applied to the signal.

Power spectra are computed at every height gate up to 350 m then averaged over five gates. Spectral slope is computed by mean square estimate. This average across vertical layers prevents assessment of the vertical variability of the spectra, but was necessary to obtain enough degrees of freedom in the spectra. It was also justified by the need to determine spectra generally representative of the mixed layer. Nevertheless, examination of height variation of spectra and/or structure functions could be possible, but using only very

* EDF: Electricité De France from Chatou.

† KNMI: Royal Meteorological Society from De Bilt, The Netherlands.

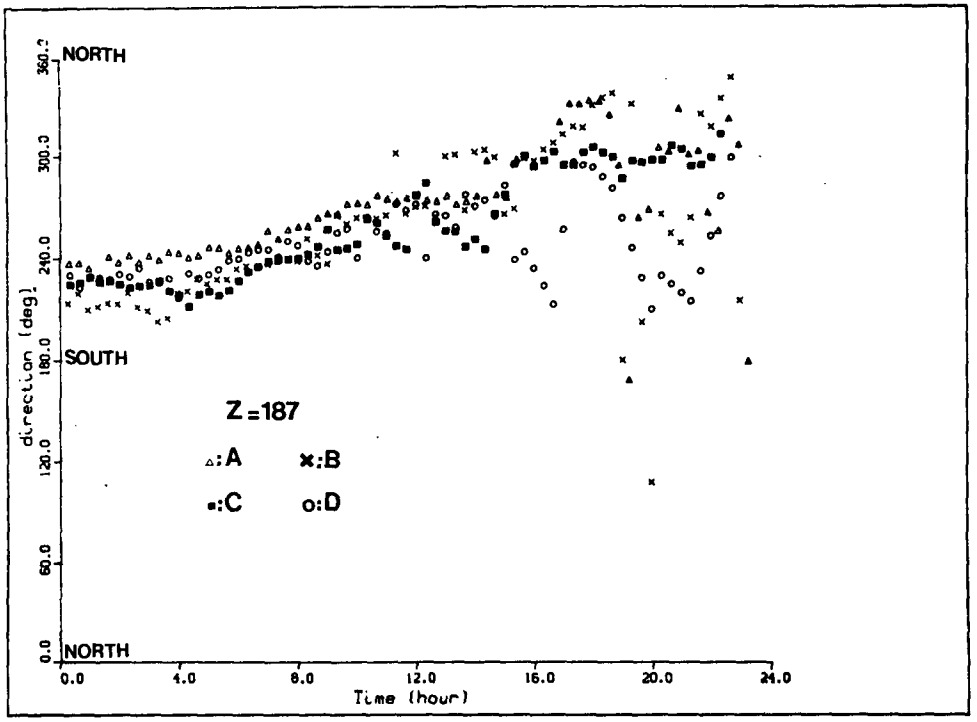

FIG. 2. (*Continued*)

limited time periods in order to increase the degrees of freedom.

Hence, for $E(k) = Ak^b$, where $E(k)$ is the spectral density and k the wavenumber, b and Δb are computed. These spectra are taken from three days of analysis and permit study of the spectral behavior from 4.1 10^{-4} Hz down to 3.9 10^{-6} Hz.

To improve the estimation and to compare spatial and temporal estimates of mesoscale turbulence behavior, temporal structure functions have also been computed for the same gates. This analysis uses four identical temporal samples for the 3 days after detrending the wind data.

The temporal structure functions are $D(\tau)$, where τ is the temporal lag [the variability is $\sqrt{D(\tau)}$]; $D(\tau)$ is also averaged on the different gates, and written as $D(\tau) = C\tau^d$.

The power law d and the differences Δd are then computed, and finally an average over the four sodars of all the estimates of the structure functions is computed, representative of a depth of 350 m height. For the spatial structure function we compute $D(\delta r)$, where one has only five spatial lags since two increments are very close to 15 km. The structure functions for the two 15 km increments have been computed and are found to give comparable amplitudes, and therefore their average is used for distance. Therefore if $D(\delta r) = E\delta r^f$, we are able to see in the case where $f \pm \Delta f$ and $d \pm \Delta d$ are not very far from each other (following Gage 1979), if there is any relationship between the spatial and temporal structure function. In this way, we can test the Taylor hypothesis. This last point is very important since it gives the link between statistics of the spatial and temporal properties of mesoscale turbulence. Gage (1979) states that "it is reasonable to use the Taylor transformation on the mesoscale," but in fact it is useful to verify this assumption.

5. Results

a. *Energy spectra*

Figures 3a–d show spectra averaged at several gates, representative of five levels. Here $nE(n)$ is plotted as a function of the frequency n. One observes a large variation of the slope in the spectral interval 8.0×10^{-6}–1.5×10^{-4} Hz. Spectral slopes range from -0.4 to -1.5, and no characteristic feature is found on the spectra, except near frequency 10^{-5} Hz where a spectral peak corresponding to a 24 h period is systematically observed on every spectrum. Spectra averaged over the four sodars and over a 350 m depth exhibit a -0.71 slope with a standard deviation of 0.30, which gives 1.75 ± 0.30 for $E(n)$ and seems to confirm, as found by Lilly and Petersen (1983) and Gage (1979), a $-5/3$ spectral behavior for $E(n)$. Larsen et al. (1982) had found slopes of -1.64 ± 0.279 and -1.604 ± 0.259 for the zonal and meridian horizontal wind components, respectively, using the same method of spectrum averaging over different gates for $E(k)$.

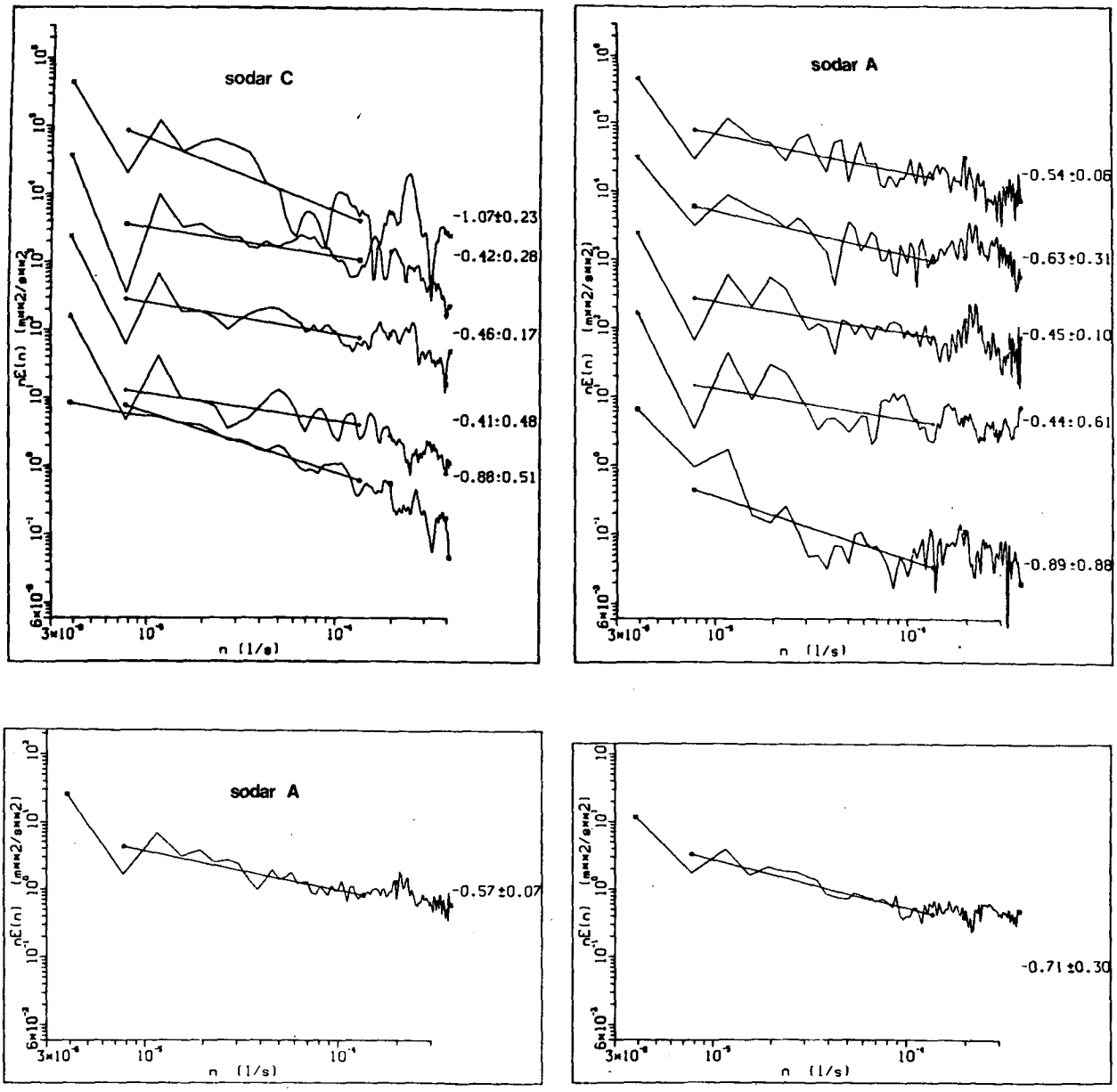

FIG. 3. (a) Wind speed energy spectra at different heights for sodar C. Spectra at successive heights have been multiplied by a factor of $10^{(k-1)}$ (with k number of levels). The amplitude is correct at level 1. (b) As in (a), but for sodar A. (c) Wind speed energy spectrum averaged over 350 m height for sodar A. (d) Wind speed energy spectrum energy averaged over 350 m for the four stations.

b. *Temporal and spatial structure functions*

Before analyzing the results from spatial structure functions, let us examine the temporal behavior using the structure function in the range 20 min up to 5 $\times 10^2$ minutes (8.3×10^{-4}–3.3×10^{-5} Hz). In Fig. 4a, a mean slope of 0.54 ± 0.1 is found, which is not very far from the $-2/3$ slope found by Gage (1979).

Looking now at the spatial structure functions at different heights for spatial increments δr of 15, 22, 25, 30, and 38 km and using four time samples of 800 min in such a way as to obtain quasi-equivalent degrees of freedom to those for the temporal structure function, we find a slope $d = 0.58 \pm 0.38$ (Fig. 4b). This result suggests that the slopes d and f are close to each other and are not fundamentally different from 2/3. However, the spectral exponent fit for the spatial structure function is, of course, not good, due to the poor number of spatial increments. Therefore, the slope and the standard deviation are compared with a Student's t distribution to see if a 2/3 slope can be considered significant. We use a two-tailed test at 0.05 and 0.70 levels

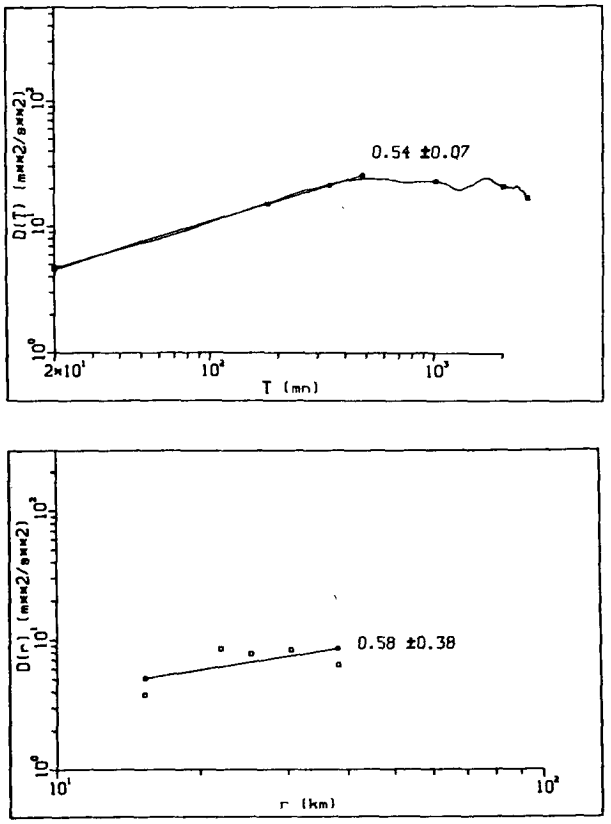

FIG. 4. (a) Temporal structure function averaged over 350 m height and over the four stations. (b) Spatial structure function averaged over 350 m height and four samples.

of significance, which shows that the sample result is probably significant.

A justification of the use of the structure function for the mean wind speed rather for the longitudinal or transverse components can be made in observing the wind direction evolution. In Fig. 2b (for day 26), we observe that the wind directions are comparable for the four sodars (uncertainty if $\pm 10°$) but the difference becomes larger during the night. Therefore, the structure function has been computed during the time period when the wind direction was similar over the four sodars. This structure function does not differ from the longitudinal structure function and the slope of 0.63 $\pm$ 0.13 in Fig. 5 shows that the previous result computed with the horizontal wind speed was not an accidental one.

Therefore, in this case $D(\tau) = C\tau^d$ and $D(\delta r) = D\delta r^f$, with d and f equal to 2/3. If τ is supposed to be equivalent to δr, using the relationship $\delta r = V\delta\tau$, we find that the ratio $D(\delta r)/D(\tau) = D/CV^{2/3}$ is best fit by 0.94 $\pm$ 0.15 with V equal to 8 m s^{-1} (Fig. 6). This value closely corresponds to the mean horizontal wind speed averaged during the three days over five heights. The horizontal wind speed ranges from 1.5 to 14 m s^{-1} with an average of 7.8 $\pm$ 2.8 m s^{-1}.

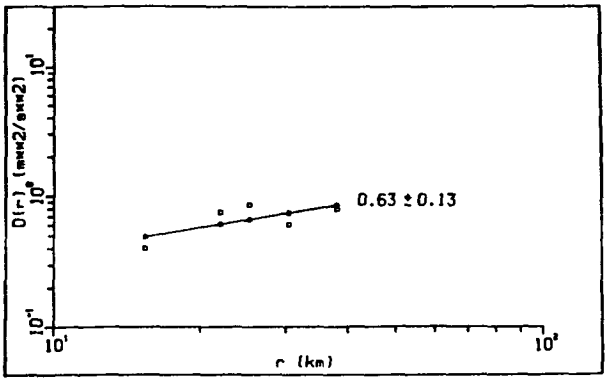

FIG. 5. Spatial structure function computed during time periods where the wind velocity direction was not very different on the four sodars.

Taking into account the different uncertainties, this result shows that, at least for a scale smaller than 38 km, the Taylor hypothesis seems to be fulfilled. The transport velocity of mesoscale turbulence corresponds to a temporal and spatial mean wind speed which approaches the mean wind speed averged during the 3 days over the four sodars.

6. Wind time series analysis; wind speed distribution function and vorticity spectra

The slope of the spectrum of the horizontal mean wind speed is found to be equal to $-5/3$. This behavior can be considered to be associated with two-dimensional mesoscale turbulence. But since a spectrum represents only a statistical point of view, no information is obtained about the flow characteristics, and the different kinds of mesoscale forcing suggested by Lilly (1983) cannot be identified. Therefore, we tried to obtain information about the evolution of the wind during the 3 days and to relate it to flow characteristics. In Fig. 7, we have plotted the wind speed as a function of time, for different heights and for wind speed class increments of 2 m s^{-1}. Wind speed at these heights is

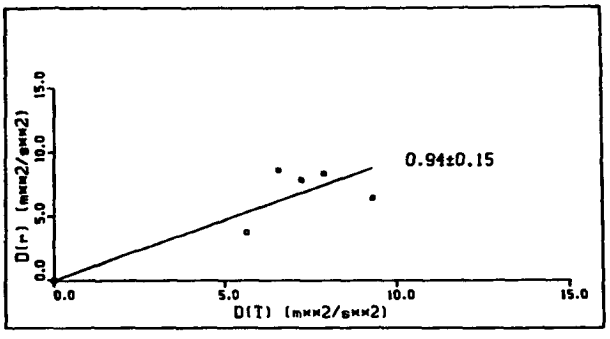

FIG. 6. Spatial structure function $D(r) = D(r)^{2/3}$ as a function of the temporal structure function $D(T) = C(r/V)^{2/3}$. The slope is indicated.

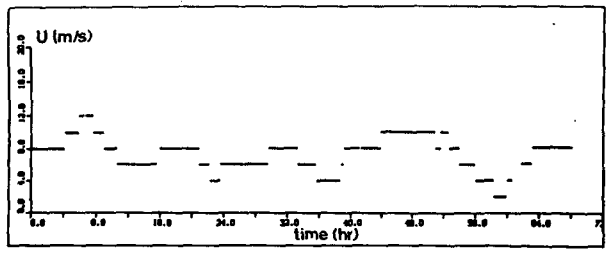

FIG. 7. Wind speed as function of time, for classes of 2 m s^{-1} over the 3 days.

large during the night and small during the day—a classical result. In each wind speed class, a mean duration of the class and a mean time interval between class events is evaluated. In Fig. 8b, on the left, one observes the mean duration and in Fig. 8a, on the right, one observes the mean time interval. It can be noticed that the mean duration for the different classes ranges from 2 to 4 h and that the mean time interval in general decreases when the wind speed class level increases. The classes corresponding to the largest period correspond to the smallest class level. Figure 7 shows that the largest period coincides with convective activity, associated with a decrease of the wind speed, an increase of the ageostrophic wind difference, and an increase in the vertical convective energy transfer. If we now plot the "pseudoperiod" (sum of mean time duration and mean time interval) (Fig. 8c), we observe a quasi-linear decrease in the wind speed class level as a function of the period, which is an illustration of the scale transition from shear production (during the night and the end of the day) toward convective transition. This result does not, a priori, have any relationship with the wind spectrum except through momentum transfer (not discussed here). Apart from convective forcing during the day and "inertial forcing" during the night, some other oscillations may be quasi-inertial oscillations, which contribute only a small fraction of the observed variance. These can appear at different levels. The temporal correlation functions in Fig. 9 show this other kind of forcing which indicates the difficulty in finding the origins of the spectral behavior.

In order to obtain statistical justification showing that the quasi-two-dimensional turbulence may be the better explanation of the spectral slope behavior, we have computed the vorticity on the surface defined by the domain of the four sodars with the method suggested by Gaynor et al. (1977). The wind circulation

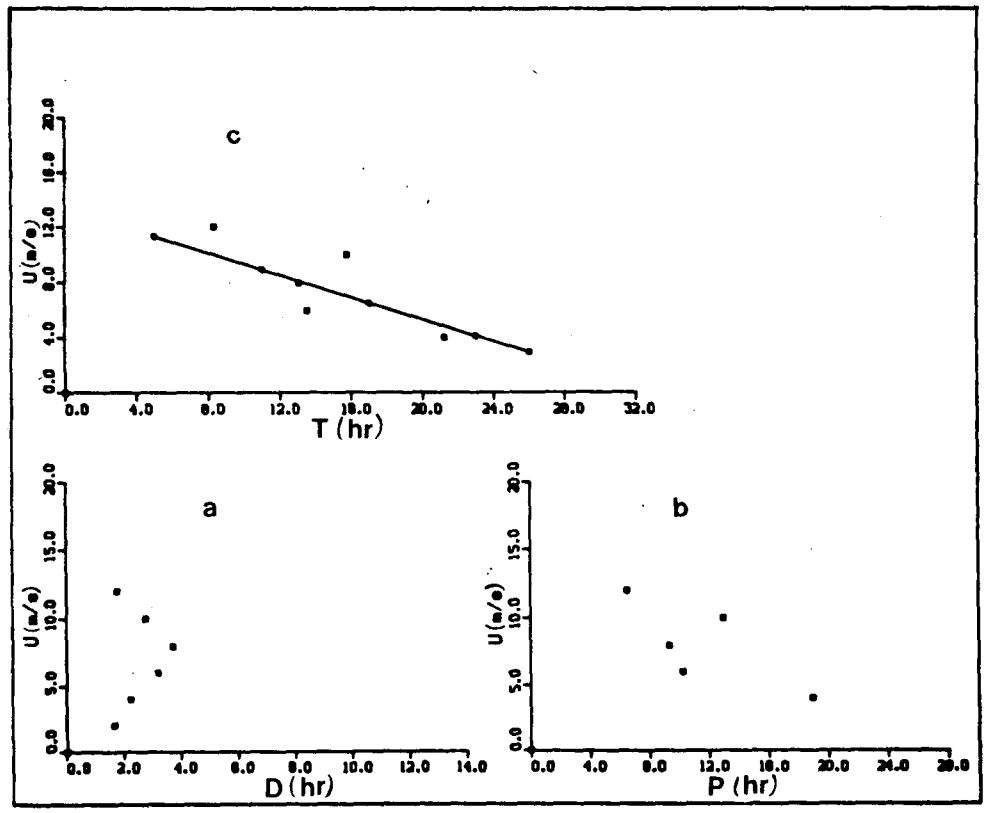

FIG. 8. (a) Mean duration (D) of each wind speed class. (b) Mean interval (P) between wind speed classes of the same magnitude. (c) Pseudoperiod ($D + P$) (mean duration of each class + mean interval between classes of the same level) for the 3 days as a function of wind speed class level.

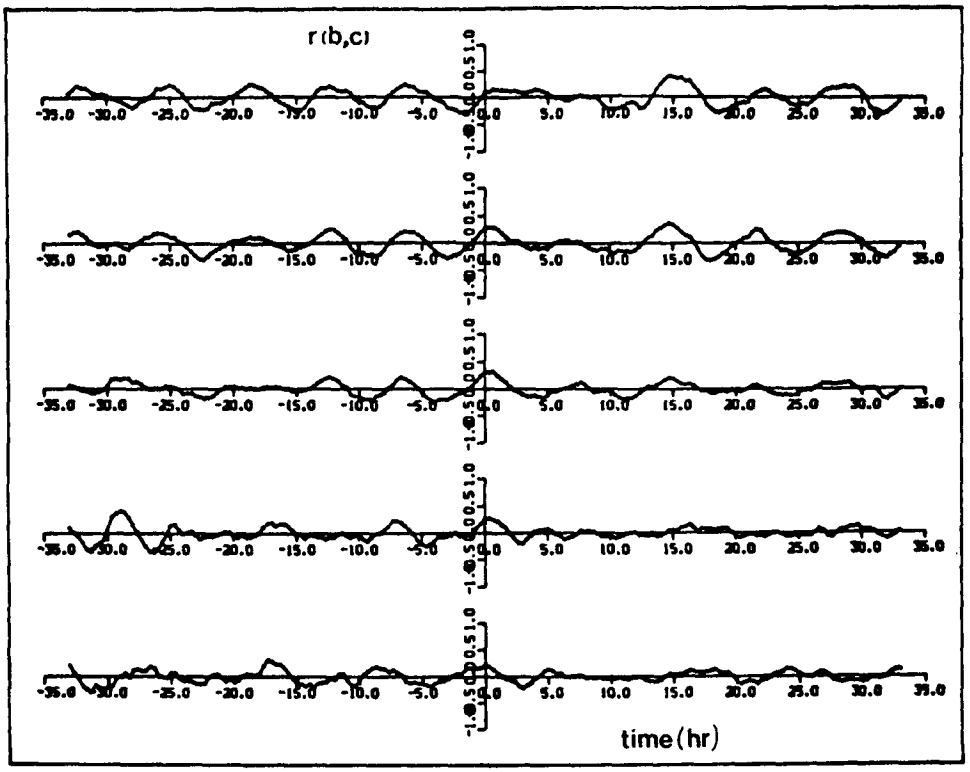

FIG. 9. Wind speed correlation function as a function of height between sodars A and B showing quasi-periodic oscillations.

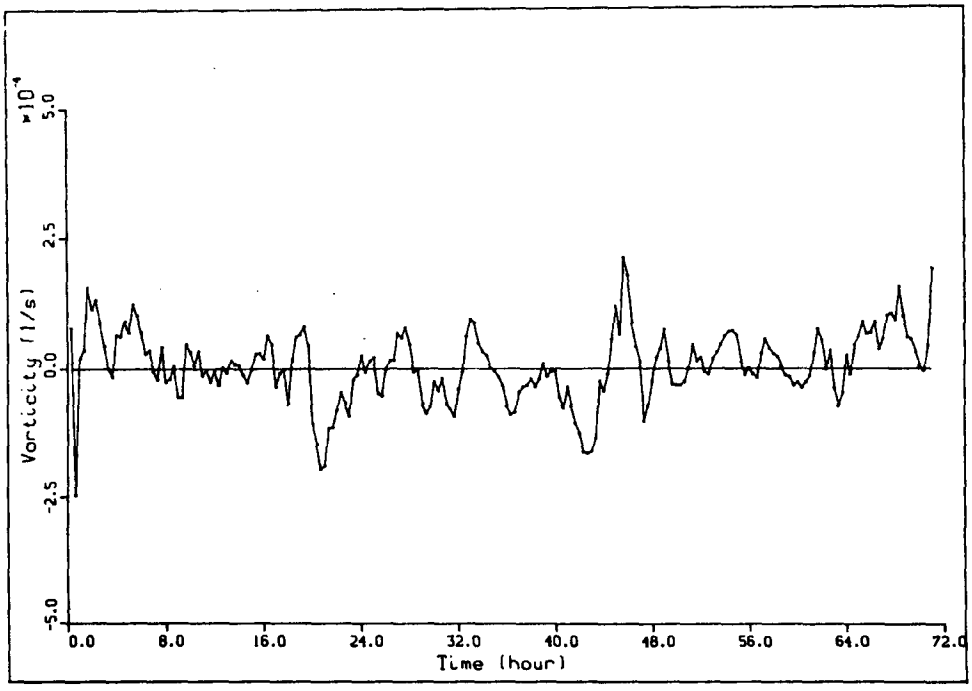

FIG. 10. Fluctuations as a function of time of the vertical component of the vorticity computed with velocity circulation using the four sodars.

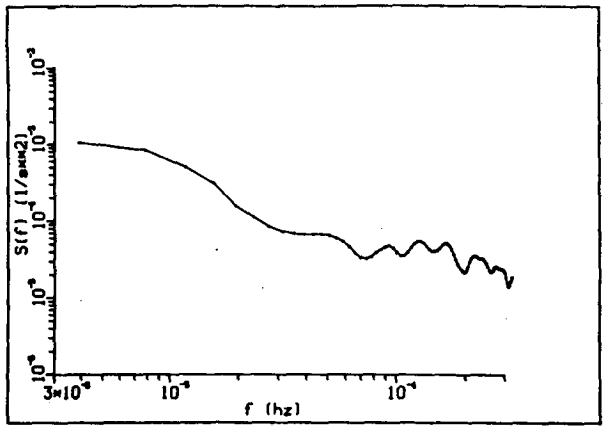

FIG. 11. Spectrum of the vertical component of vorticity as a function of frequency.

around the domain is calculated and the wind components between the different sodars are interpolated. This method gives Fig. 10, as a function of time, the vorticity fluctuations in a domain only representative of surface around the four stations. Figure 11 shows a vorticity spectrum which gives a clear indication that the vorticity variance at low frequencies of the spectrum is rather large. This is more a justification of the assumption of two-dimensional turbulence rather than the assumption of turbulence related to gravity wave production. The spectral slope in Fig. 11 has no relevance due to the low precision in the vorticity estimate and the filtering effect due to the surface dimension in which the vorticity has been computed.

7. Conclusions

Summarizing the different results, we have analyzed wind speed as obtained by four Doppler sodars every 20 min in the clear atmospheric boundary layer and have found that the spectrum of mean wind speed follows a $-5/3$ spectral law. This result seems, for the sample used during these 3 days of observation, to be justified more by quasi-two-dimensional turbulence than by a theory based on gravity wave dispersion.

An analysis of spatial and temporal structure functions with spatial increments limited to 38 km has shown the validity of Taylor's hypothesis at this scale; the turbulence advection speed has been found to be very close to the mean spatial wind speed averaged over the four sodars and over the sample duration. This result is indeed very important for mesoscale turbulence modeling, and suggests further measurements with sodars, using a larger variety of spatial increments.

Interpretation of spectral behavior has been clarified by analysis of the wind speed distribution using speed classes of 2 m s^{-1}. The observations show that the different classes could be related to the following phenomena, inertial effects and convective forcing. However, temporal correlation functions suggest the presence of oscillations and/or gravity waves.

Combining a sodar network with a tropospheric radar network would make it possible to analyze the behavior with height of the mesoscale turbulence.

Acknowledgments. The authors would like to thank all their colleagues who have participated in the Mesogers experiment, especially F. Baudin, J. F. Fèvre, J. Bilbille, A. Sauvaget, J. P. Vinson and B. Piron. Special thanks are due to E.D.F. for experimental support with the E.D.F. Doppler sodar, and to K.N.M.I. for its participation to Mesogers experiment. Many thanks are also due to C. Mazaudier for preparing the Mesogers data base.

This experiment has received support from I.N.S.U. (C.N.R.S.) and C.N.E.T.

REFERENCES

Chong, M., 1976: Mesure des profils de vent par Sodar Doppler. *Note Technique CRPE,* **22,** 103.

Desbois, M., 1975: Large-scale kinetic energy spectra from Eulerian analysis of Eole wind data. *J. Atmos. Sci,* **32,** 1838–1847.

Dickey, T. D., and G. L. Mellor, 1980: Decaying turbulence in neutral and stratified fluids. *J. Fluid Mech.,* **99,** 13–31.

Gage, K. S., 1979: Evidence for $k^{-5/3}$ law inertial range in mesoscale two dimensional turbulence. *J. Atmos. Sci.,* **36,** 1950–1954.

——, and W. H. Jasperson, 1979: Mesoscale wind variability below 5 km as revealed by sequential high-resolution wind soundings. *Mon. Wea. Rev,* **107,** 77–89.

Garrett, C., and W. Munk, 1979: Internal waves in the ocean. *Annu. Rev. of Fluid Mech.* **11,** 339–369.

Gaynor, J. E., F. F. Hall Jr., J. G. Edinger and G. R. Ochs, 1977: Measurement of vorticity in the surface layer using an Acoustic Echo Sounder Array. *Remote Sen. Environ. Sci.* **6,** 127–137.

Julian, P. R., W. M. Washington, L. Hembree and C. Ridley, 1970: On the spectral distribution of large-scale atmospheric kinetic energy. *J. Atmos. Sci.* **27,** 376–387.

Kraichnan, R. H., 1967: Inertial ranges in two-dimensional turbulence. *Phys. Fluids,* **10,** 1417–1423.

Larchevèque, M., 1981: Contributions à l'étude de la diffusion d'un contaminant passif par une turbulence de grille soumise à une déformation plane. Thèse de doctorat d'Etat, Université Paris VI.

Larsen, M. F., M. C. Kelley and K. S. Gage, 1982: Turbulence spectra in the upper troposphere and stratosphere between 2 hours and 40 days. *J. Atmost. Sic.* **39,** 1035–1041.

Leith, C. E. and R. H. Kraichnan, 1972: Predictability of turbulent flows. *J. Atmos. Sci.,* **29,** 1040–1058.

Lesieur, M., 1983: Introduction à la turbulence bidimensionnelle. *J. Méc. Théorique et Appliquée,* **0750-7240,** 5–20.

Lilly, D. K., 1969: Numerical simulation of two-dimensional turbulence. *Phys. Fluids,* **Supplement II,** 240–249.

——, and E. Petersen, 1983: Aircraft measurements of atmospheric energy. *Tellus,* **35A,** 379–382.

——, 1983: Stratified turbulence and the mesoscale variability of the atmosphere. *J. Atmos. Sci.,* **40,** 749–761.

——, 1984: The mesoscale "noise" spectrum of the atmosphere: Wave or turbulence? (Notes by S. Garner and K. Sangren), *Summer School on Mesoscale Meteorology* (NCAR), W. Klemp, Ed., 355–364.

Lorenz, E. N., 1969: The predictability of a flow which processes many scales of motion. *Tellus,* **21,** 289–307.

Morel, P., and M. Larchevèque, 1974: Relative dispersion for constant-level balloons in the 200 mb general circulation. *J. Atmos. Sci.,* **31,** 2189–2196.

Nastrom, G. D., and K. S. Gage, 1983: A first look at wave number spectra from GASP data. *Tellus*, **35A**, 383–388.

——, and K. S. Gage, 1984: A climatology of atmospheric wave spectra of wind and temperature observed commercial aircraft. *J. Atmos. Sci.*, **42**, 950–960.

Papoulis, A., 1973: Minimum-bias windows for high-resolution spectral estimates. *IEEE Trans. Inf. Theory*, **19**, 9–12.

Spizzichino, A., 1974: Discussion of the operating conditions of a Doppler sodar. *J. Geophys. Res.* **79**, 5585–5591.

Tatarskii, V. I., 1961: Wave propagation in a turbulent medium (translated by R. A. Silvermann), McGraw-Hill, 285 pp.

VanZandt, T. E., 1982: A universal spectrum of buoyancy waves in the atmosphere. *Geophys. Res.*, **9**, 575–578.

Weill, A. F., C. Baudin, C. Klapisz, J. P. Goutorbe, P. Van Grunderbeeck and P. Leberre, 1978: Turbulence structure in temperature inversion and in convection fields as observed by Doppler sodar. *Bound. Lay. Meteor.*, **15**, 375–390.

——, C. Klapisz, B. Strauss, F. Baudin, C. Jaupart, P. Van Grunderbeeck and J. P. Goutorbe, 1980: Measuring heat flux and structure functions of temperature fluctuations with an acoustic Doppler sodar. *J. Appl. Meteor.*, **19**, 199–205.

——, C. Mazaudier, C. Kapisz, F. Leca, M. Masmoudi, D. Vidal-Madjar, R. Bernard, O. Taconet, B. S. Gera, A. Sauvaget, A. Druilhet, G. Dubosclard, J. Y. Caneill, P. Mery, A. G. M. Beljaars, W. A. A. Monna, J. G. Van Der Vliet, M. Crochet, D. Thomson and T. Carlson, 1987: Mesogers 84 experiment: a report. *Bound. Lay. Meteor.*, **42**, 251–264.